Analysis of Insect and Plant Colors in Digital Images Using Java Software on the Internet

JOHN A. BYERS[1]

Western Cotton Research Laboratory, USDA–ARS, 4135 East Broadway Road, Phoenix, AZ 85040

Ann. Entomol. Soc. Am. 99(5): 865–874 (2006)

ABSTRACT Description of colors of insects and plants in biological research is often subjective and imprecise. A quantitative, statistical, and standardized method for describing colors by software analysis of digital images would be useful to researchers if readily available. An Internet Web page with JavaScript and Java applet was made that loads a digital image and analyzes the red, green, and blue (RGB) intensity components of the pixels in any rectangular area of relatively uniform color. A mean, standard deviation (SD), coefficient of variation, and percentage of each of the three color components in the area is calculated. Thus, a colored area in an image can be depicted objectively as R ± SD, G ± SD, and B ± SD, or percentages thereof, allowing mean color to be reproduced elsewhere by paint programs. For each analysis, the software uses the RGB component colors to make a bar graph with each RGB value and SD. The software was used to analyze colors of flowers and leaves of two cotton species, white and red varieties of upland, *Gossypium hirsutum* L., and Pima, *Gossypium barbadense* L. (Malvaceae); western tarnished plant bug, *Lygus hesperus* Knight (Heteroptera: Miridae); yellow plastic used in insect traps; and eight other insect species. Three two-dimensional (2D) color-space diagrams (hexagon, 2D-cube, and ternary percentages) are described and used to plot colors from analyses. Statistical tests are presented that compare whether two groups of color-space points in three dimensions are significantly separated. Differences in color vision are compared in humans, insects, digital cameras, and spectroradiometers.

KEY WORDS color analysis, RGB, cotton, vision, image analysis

Since 1970, there have been >2,700 research articles concerning insects in which color is described or considered, with numerous reports containing subjective descriptions of color (BIOSIS Previews, Philadelphia, PA). Although a spectroradiometer can measure wavelengths of reflected colors objectively, there are still many recent reports of color assessments by human observers. For example, no instruments were used in defining colors of plants and fruits attractive to insects (Bohac et al. 2002, Kelley et al. 2002, Marchand and McNeil 2004, Whitney and Stanton 2004), colors of insect bodies (Tanaka 2000, Appleby and Credland 2001, Braendle and Weisser 2001, Wang 2002, Zhao et al. 2003), or colors of insect traps (Hoback et al. 1999, Howarth and Howarth 2000). The spectroradiometer is commonly used to record the wavelengths in a spectrum of light reflected from an object. However, use of a spectroradiometer has several drawbacks: 1) the instrument is expensive (>$3,500); 2) it requires connection to a portable computer; 3) it usually averages reflectance from areas larger than an insect; and 4) it is difficult to recreate a color, as understood by humans or insects, from the wavelength data represented as a graph of intensity versus wavelength.

Researchers may describe species of insects using colors that are not only subjective but also may vary due to cultural and language differences (Zollinger 1988, Saunders and van Brakel 1989, Byers 1996, Mausfeld 2003). The description of color by humans can also vary due to red-green color "blindness" (6–8% of males) or more subtle, but common, differences in wavelength sensitivity in the red-absorbing color pigments in the cones of human eyes (Merbs and Nathans 1992, Winderickx et al. 1992). Thus, it would be useful in research to have an inexpensive and readily available method that can describe colors of organisms objectively and quantitatively, such as might occur during growth and development or under different environmental conditions.

Digital cameras are increasingly consistent and accurate in color replication as specified by the International Color Consortium (http://www.color.org), the International Organization for Standardization (ISO), and the International Electrotechnical Commission (IEC) (Baxes 1994). Trzoniec (2005) reports that 10 yr ago, digital cameras were more expensive and had poor quality compared with film, but today

[1] Current address: U.S. Arid-Land Agricultural Research Center, USDA–ARS, 21881 North Cardon Lane, Maricopa, AZ 85239 (e-mail: jbyers@wcrl.ars.usda.gov).

"picture quality is now on a par with film." Many brands of digital cameras can capture large images that are translated into digital images stored in memory as files that can be formatted either directly or by software to Joint Photographic Experts Group (JPEG) images, often ending in *.JPG (Baxes 1994). The Internet Web browsers use JPG and GIF (Graphics Interchange Format, CompuServe) files to show images, with JPG being more realistic in representing natural scenes because of the ability to show higher numbers of colors together in an image. In both image file formats, picture elements (pixels) make up the images, and the pixels are colored based on an RGB (red, green, blue) system where each pixel combines the three components in ranges from 0 to 255 in intensity. This means each pixel can potentially have 256^3 = 16,777,216 different colors, or shades thereof. Specifying a color of R = 255, G = 255, and B = 0 would yield a bright yellow, whereas darker, less brilliant shades of yellow can be made by decreasing equally the values of R and G. Therefore, any color or shade of color can be reproduced reliably with the RGB system, the most common color system used by personal computers.

My objective was to use the ubiquitous and relatively inexpensive digital camera to capture light images of biological samples in real time and then analyze the images by algorithms implemented by the Java programming language (Sun Microsystems Inc., Santa Clara, CA) run under Web browsers such as Internet Explorer (Microsoft. Redmond, WA). The Internet-based analysis system can be downloaded and run on a web browser offline on personal computers (Byers 2002). I envisioned software that loads a digital image, allows a rectangular area of the image to be selected with the mouse, and then this area's pixels are analyzed for their red, green and blue intensity components (RGB), each with a mean and standard deviation (SD). The average RGB values or their trichromatic percentages are an objective analytical description of the color obtained from a specific area of an object. The values then could be referenced in publications without resorting to color photos. Colors could be reproduced via screen or printing for use in experiments on animal behavior. The method should give meaningful results as long as the sampled areas are relatively uniform and do not cover complex color patterns.

A second objective was to investigate graphical color-space models and devise statistical tests to compare RGB colors obtained by the software for differences between groups of plants or insects. Specifically, color descriptions of insects and trap materials were compared to test for significant differences between the sexes of plant bugs and varieties and ages of cotton flowers and leaves. I also wanted to compare reflected wavelengths of various objects measured by a spectroradiometer to corresponding images made by several digital camera models and observe the variation in RGB values.

Materials and Methods

Software in the form of an Internet Web page (rgb.htm) was constructed using the JavaScript (Goodman 1996) and HTML (Stanek 1996) programming languages as well as a Java applet (rgb.class) coded in the Java language (http://java.sun.com, Sun Microsystems Inc.). The Web page and applet are viewed by current versions of Netscape or Internet Explorer (IE) and can be viewed as a demo at the Internet site http://www.chemical-ecology.net/java2/rgb.htm. However, to analyze personal images the software must be downloaded from the site to a personal computer, and the files must be placed in a directory java2 with images for analysis in a subdirectory of java2 (e.g., graphs) and then rgb.htm opened by one of the Web browsers mentioned above. This is because Java applets loaded from another Internet site will not access files on a personal computer because of security reasons.

To use the software (Fig. 1), the user enters the filename of an image to be analyzed as well as an optional subdirectory name. After an image name is entered, the [Start Analysis] button is clicked, which loads and shows the image (up to 3,400 by 3,400 pixels). The mouse is used to select a rectangular area of the image for analysis by moving to an upper left corner of the desired area, clicked to start a blinking rectangular-box outline, moved to enlarge the box, and then clicked again when the desired area is surrounded by the box. If a new analysis area is desired, the mouse is clicked again to erase the box, and then the process repeated. Fine control of the box location/size can be done with the keyboard keys "left/right arrows" for the right and "up/down arrows" for the bottom line of the box, whereas the "Home/End" keys are used to move the top line and the "Delete/Page Down" keys for the left line of the box. When ready, the user presses the "Esc" key and the area immediately turns red and the analysis results are shown in the status bar.

In addition, below the image in the browser a graph is shown (Fig. 2) with RGB values as colored bars and lines of each SD. The graph also reports the coordinates of the area, the number of pixels analyzed, the means of R, G, and B values (0–255) each with ±SD and coefficient of variation (coefficient of variation, SD/mean × 100, Sokal and Rohlf 1995). The trichromatic percentages of each of the values in the ternary mixture also are calculated [e.g., $R\% = R/(R+G+B) \times 100$].

Various natural objects in the field were photographed with a Nikon Coolpix 2100 digital camera at the macro setting and 1,600 by 1,200 pixel resolution, and the resulting JPEG images analyzed for color with the software described above. A plant gall of *Adelges cooleyi* (Gillette) (Homoptera: Adelgidae = Chermidae) on Engelmann spruce, *Picea engelmannii* Parry ex Engelmann (Pinaceae), was photographed 12 August 2004 (Latir peak, NM). The yellowish white flowers of upland cotton, *Gossypium hirsutum* L. (Malvaceae), were photographed at 1400 hours under sunlight (17–18 August 2004), with the withering flowers on the second day having a distinct pinkish tinge. The flowers and leaves of two *G. hirsutum* varieties (red and white flowers) and Pima cotton, *Gossypium barbadense* L. (yellow flowers), also were photographed at the same time. The western tarnished plant bug, *Lygus hesperus* Knight (Heteroptera: Miridae), reared

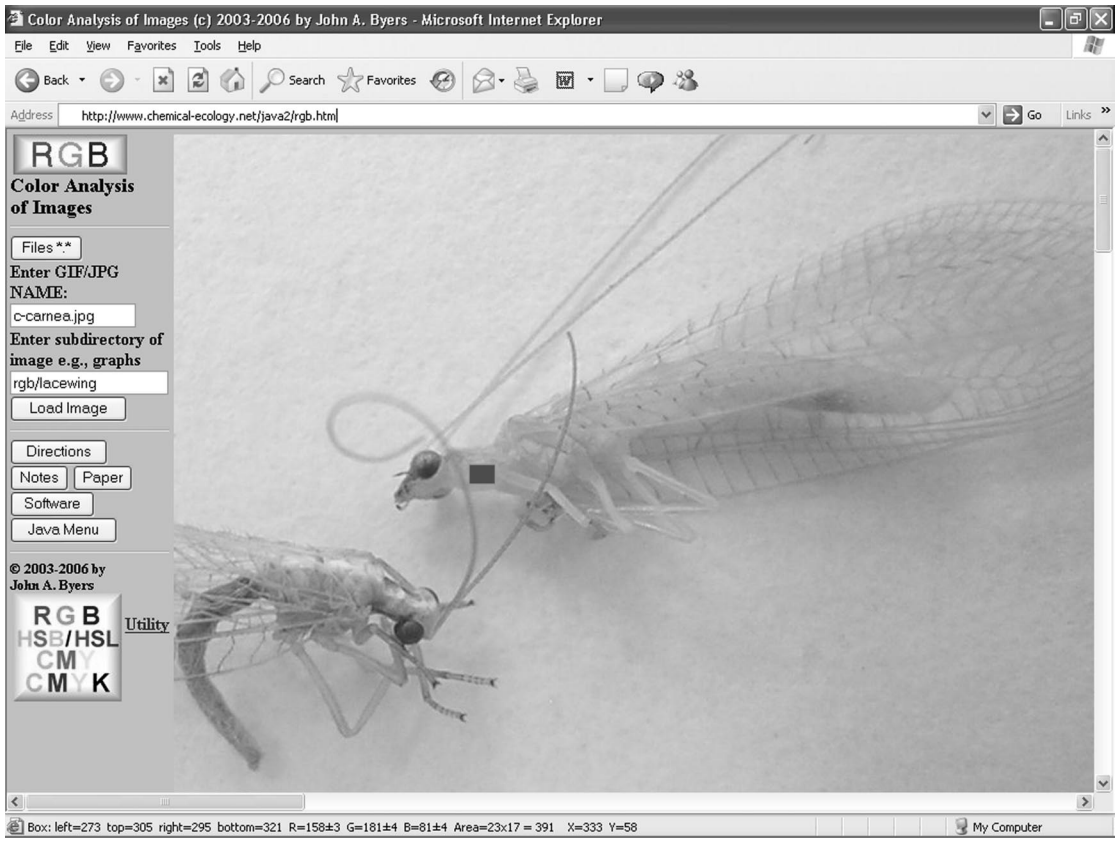

Fig. 1. Screen capture image of Internet Explorer browser with HTML Web page and JavaScript controls on left used to control a Java applet that loads an image of lacewings in which the prothoracic area of one is analyzed (black rectangle of 391 pixels) for RGB colors with results reported in the status bar at bottom (the results also are reported in two graphs under the image but not visible without scrolling).

in the laboratory (Blackmer et al. 2004), and green lacewings, *Chrysoperla carnea* (Stephens) (Neuroptera: Chrysopidae), were photographed in the laboratory under a combination of white LED and fiber optic tungsten lighting. Images of various yellow-colored plastic sheets used for insect sticky-traps (Pestick sheeting, Hummert International, Earth City, MO) and yellow and green papers (Post-It, 3M, St. Paul, MN) also were photographed in sunlight and analyzed with the software. Several insects (species in Table 2) in forests of Sweden and California were photographed with a Minolta 600si SLR camera by using a 90-mm Tamron macro-lens on 35-mm slide film (Kodak Ektachrome 100, Eastman Kodak, Rochester, NY). The slides were later scanned with an Olympus ES-10 film scanner (Olympus, Melville, NY), and various solid colors in the resulting JPG images were processed with the RGB software.

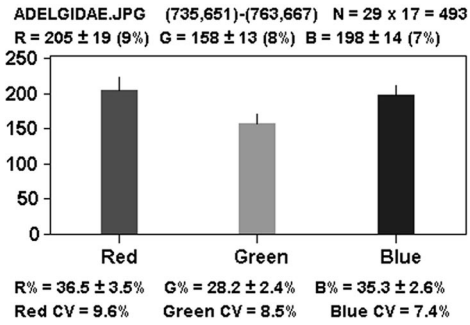

Fig. 2. Color analysis of an insect gall caused by *A. cooleyi* on Engelmann spruce twig showing details of the SD, coefficient of variation, and percentages of color intensity components as drawn by the software.

To assess the variation in RGB analyses of images taken with different digital cameras, 8 by 11 sheets of purple or red construction paper were photographed with five digital camera models under overcast skies (≈40,000 lux) and compared with corresponding reflectance spectra from a USB2000 spectroradiometer using OOIBase32 version 2.0.2.2 software (Ocean Optics Inc., Dunedin, FL). At the same time, the two sheets of yellow insect-trap plastic described above were analyzed by the spectroradiometer and the Nikon 2100. Another comparison between the spectroradiometer and the RGB method was done with flowers and leaves of upland cotton in sunlight.

Table 1. Mean RGB values and trichromatic percentages from areas of digital photos of cotton flowers and leaves analyzed by the Java software

Sample description	Pixels[a]	R ± SD (CV) R %[b]	G ± SD (CV) G %	B ± SD (CV) B %
Upland cotton, *G. hirsutum*				
White flower petal A	1,971	235 ± 4 (2) 37.4	231 ± 4 (2) 36.7	163 ± 6 (4) 25.9
White flower petal B	1,116	241 ± 2 (1) 39.7	238 ± 4 (2) 39.2	128 ± 7 (6) 21.1
White flower petal C	1,800	233 ± 6 (3) 38.1	235 ± 8 (3) 38.5	143 ± 9 (6) 23.4
White flower petal D	1,833	223 ± 5 (2) 36.7	224 ± 6 (3) 36.8	161 ± 3 (2) 26.5
Day old white flower A	4,048	222 ± 12 (5) 39.9	161 ± 19 (12) 29.0	173 ± 14 (8) 31.1
Day old white flower B	1,813	235 ± 7 (3) 38.6	195 ± 10 (5) 32.0	179 ± 9 (5) 29.4
Day old white flower C	2,442	229 ± 12 (5) 39.8	180 ± 18 (10) 31.2	167 ± 13 (8) 29.0
Day old white flower D	5,022	241 ± 6 (2) 43.0	176 ± 9 (5) 31.4	144 ± 7 (5) 25.7
Red flower petal A	3,750	249 ± 10 (4) 59.0	74 ± 20 (27) 17.5	99 ± 19 (20) 23.5
Red flower petal B	3,555	240 ± 13 (6) 55.6	72 ± 14 (20) 16.7	120 ± 13 (10) 27.8
Red flower petal C	6,930	230 ± 20 (9) 62.8	50 ± 26 (52) 13.7	86 ± 23 (26) 23.5
Red flower petal D	6,206	247 ± 10 (4) 54.0	88 ± 19 (21) 19.3	122 ± 13 (11) 26.7
Pima cotton, *G. barbadense*				
Yellow flower petal A	2,350	234 ± 4 (2) 41.9	241 ± 5 (2) 43.0	85 ± 8 (10) 15.2
Yellow flower petal B	3,025	228 ± 6 (3) 43.4	225 ± 8 (4) 42.9	72 ± 11 (16) 13.7
Yellow flower petal C	2,184	230 ± 4 (2) 46.0	218 ± 8 (4) 43.6	52 ± 8 (15) 10.4
Yellow flower petal D	2,268	227 ± 4 (2) 41.2	236 ± 3 (2) 42.8	88 ± 6 (7) 16.0
Leaves of cotton				
G. hirsutum (green) A	2,170	91 ± 7 (7) 31.8	125 ± 6 (5) 44.1	69 ± 7 (10) 24.1
G. hirsutum (green) B	2,627	111 ± 13 (12) 34.5	160 ± 13 (8) 49.7	51 ± 11 (22) 15.8
G. hirsutum (green) C	1,240	52 ± 5 (10) 31.3	93 ± 5 (5) 56.0	21 ± 5 (24) 12.7
G. hirsutum (green) D	1,656	64 ± 8 (12) 30.9	99 ± 8 (8) 47.8	44 ± 9 (20) 21.3
G. barbadense (green) A	2,200	98 ± 4 (4) 32.3	134 ± 4 (3) 44.2	71 ± 7 (10) 23.4
G. barbadense (green) B	2,397	92 ± 5 (5) 34.3	126 ± 4 (3) 47.0	50 ± 5 (10) 18.7
G. barbadense (green) C	2,156	79 ± 12 (15) 36.6	113 ± 12 (11) 52.3	24 ± 13 (54) 11.1
G. barbadense (green) D	2,784	91 ± 8 (9) 32.6	140 ± 6 (4) 50.2	48 ± 12 (24) 17.2
G. hirsutum (red variety) A	3,082	170 ± 16 (9) 38.3	139 ± 19 (14) 31.3	135 ± 15 (11) 30.4
G. hirsutum (red variety) B	2,322	159 ± 7 (4) 37.0	133 ± 9 (7) 30.9	138 ± 8 (6) 32.1
G. hirsutum (red variety) C	5,600	133 ± 11 (8) 38.3	110 ± 16 (14) 31.7	104 ± 13 (12) 30.0
G. hirsutum (red variety) D	6,177	147 ± 13 (9) 35.9	131 ± 14 (11) 32.0	132 ± 14 (11) 32.2

[a] Area analyzed in pixels (n of sample).

[b] Represents the R (red intensity) ± SD (standard deviation) [CV, coefficient of variation defined as SD/R × 100) and percent red (R/(R + G + B) × 100]. G and B defined similarly.

Chittka (1996) describes a way to plot colors graphically in a hexagonal color space. The RGB values, which can be thought of as values in three dimensions (x, y, z), are converted to x, y coordinates in two-dimensions according to the following formula as modified slightly:

$$x = \sqrt{3}/2 \cdot (R/255 - B/255) \cdot s + x_c \text{ and}$$
$$y = (G/255 - 0.5 \cdot (R/255 + B/255)) \cdot s + y_c \quad [1]$$

where R, G, and B are the RGB values, s is the size of the diagram, and x_c, y_c is the position of the hexagon on the paper. I devised a second way of depicting colors graphically in a cubic color space as transformed to two-dimensions. The coordinates are given by:

$$x = ((R/255 + 0.5 \cdot B/255) - 0.5) \cdot s \cdot \sqrt{2} + x_c \text{ and}$$
$$y = ((G/255 + 0.5 \cdot B/255) - 0.5) \cdot s \cdot \sqrt{2} + y_c \quad [2]$$

A third method is that of the standard ternary diagram where the proportions (or percentages) of the colors are plotted along the three bisecting axes of an equilateral triangle. The RGB values must first be converted to percentages, $a = R/(R + G + B)$, $b = G/(R + G + B)$ and $c = B/(R + G + B)$. Then the x, y coordinates are obtained from geometry (equations in Byers 1992) as the intersection of two lines representing two of the three proportions because c is always equal to $1 - (a + b)$. One line is parallel to the triangle side of the base of R and intersects the perpendicular bisector axis from the base to the vertex of R at the value of a, whereas the other line corresponds similarly to G and b.

A statistical method was developed to determine whether two groups of data were significantly separated from each other in the three-dimensional (3D) color space. As Chittka (1996) stated, the RGB values can be represented in a 3D space of R, G, and B directions. Thus, the nonredundant distances between color points can be calculated with the Pythagorean formula [$d = \text{SQRT}((R_1 - R_2)^2 + (G_1 - G_2)^2 + (B_1 - B_2)^2)$] among all points within each group (e.g., for four points there are six distances). The variance of the distances can then be calculated and the group with the greater variance should be selected as group 1 and have distances calculated between each of its points and all other points in the other group (e.g., for four in group 1 and 4 in group 2 there are 16 intergroup distances). Then, a t-test for homogeneous variances was done to compare the mean of the distances for group 1 (group with larger variance) and the mean for the intergroup distances.

Table 2. Mean RGB values and trichromatic percentages from areas of digital photos of insects and colored trap materials analyzed by the Java software

Sample description	Pixels[a]	R ± SD (CV) R %[b]	G ± SD (CV) G %	B ± SD (CV) B %
L. hesperus[c]				
Female ventral abdomen A	168	92 ± 5 (5) 39.1	106 ± 4 (4) 45.1	37 ± 5 (13) 15.7
Female ventral abdomen B	468	124 ± 7 (6) 41.9	131 ± 6 (4) 44.3	41 ± 9 (21) 13.9
Female ventral abdomen C	272	101 ± 4 (4) 39.9	112 ± 4 (4) 44.3	40 ± 4 (10) 15.8
Female ventral abdomen D	224	84 ± 10 (12) 34.3	108 ± 7 (7) 44.1	53 ± 8 (14) 21.6
Male ventral abdomen A	88	183 ± 8 (5) 43.2	170 ± 8 (5) 40.1	71 ± 6 (8) 16.7
Male ventral abdomen B	299	173 ± 7 (4) 46.4	150 ± 6 (4) 40.2	50 ± 6 (12) 13.4
Male ventral abdomen C	192	152 ± 6 (4) 46.6	134 ± 6 (5) 41.1	40 ± 4 (11) 12.3
Male ventral abdomen D	288	180 ± 12 (7) 42.3	162 ± 13 (8) 38.0	84 ± 14 (16) 19.7
C. carnea female[d]				
Prothroax (−10 under exposed)	391	108 ± 3 (3) 40.3	130 ± 4 (3) 48.5	30 ± 4 (13) 11.2
Prothorax (0 normal exposure)	Same	133 ± 3 (2) 38.8	155 ± 4 (3) 45.2	55 ± 4 (7) 16.0
Prothorax (+10 over exposure)	Same	158 ± 3 (2) 37.8	180 ± 4 (2) 43.1	80 ± 4 (5) 19.1
Insect trap and paper materials[e]				
Yellow plastic sheet A	1,216	206 ± 1 (1) 46.1	201 ± 1 (1) 45.0	40 ± 1 (3) 8.9
Yellow plastic sheet B	1,216	194 ± 2 (1) 51.1	171 ± 1 (1) 45.0	15 ± 2 (11) 3.9
3M Post-It green paper	1,216	191 ± 1 (1) 38.5	226 ± 1 (1) 45.6	79 ± 2 (2) 15.9
3M Post-It yellow paper	1,216	207 ± 2 (1) 43.7	195 ± 2 (1) 41.1	72 ± 2 (3) 15.2
White paper	1,216	212 ± 3 (2) 33.2	214 ± 3 (1) 33.5	213 ± 3 (1) 33.3
Scanned 35-mm slides of insects[f]				
Skipper butterfly forewing	435	203 ± 8 (4) 56.5	117 ± 6 (5) 32.6	39 ± 4 (10) 10.9
Clerid beetle prothorax	255	175 ± 9 (5) 59.5	84 ± 14 (16) 28.6	35 ± 18 (50) 11.9
Red wood ant prothorax	437	169 ± 15 (9) 70.4	38 ± 29 (75) 15.8	33 ± 15 (45) 13.8
Cerambycid beetle elytron	1,665	110 ± 42 (38) 40.3	88 ± 46 (51) 32.2	75 ± 46 (61) 27.5
Tiger beetle elytron	1,500	83 ± 13 (15) 36.2	95 ± 12 (13) 41.5	51 ± 11 (22) 22.3
Bark beetle adult, head gula	696	92 ± 11 (12) 96.8	1 ± 2 (170) 1.1	2 ± 3 (116) 2.1
Bark beetle callow, head gula	690	219 ± 4 (2) 60.0	100 ± 4 (4) 27.4	46 ± 5 (10) 12.6

[a] Area analyzed in pixels (*n* of sample).

[b] Represents the R (red intensity) ± SD (standard deviation) [CV, coefficient of variation defined as SD/R × 100) and percent red (R/(R + G + B) × 100]. G and B defined similarly.

[c] Ten-day-old adults from laboratory culture, Maricopa, AZ.

[d] September 2004, Maricopa, AZ.

[e] All materials in same photo in sunlight.

[f] Insects as listed: *Ochlodes venatus* (Bremer & Grey) (Lepidoptera: Hesperiidae; June 1999, Torsby, Sweden); *Thanasimus formicarius* L. (Coleoptera: Cleridae; June 1999, Torsby, Sweden); *Formica aquilonia* Yarrow (Hymenoptera: Formicidae; June 1999, Torsby, Sweden); *Acanthocinus aedilis* L. (Coleoptera: Cerambycidae; April 1999, Lund, Sweden); *Cicindela campestris* L. (Coleoptera: Cicindelidae; June 1999, Torsby, Sweden); *I. paraconfusus;* August 1985, Bass Lake, CA), adult recently emerged from log, callow dissected from under bark.

Results

Rectangular areas of pixels that seemed a homogenous color in the digital photos were chosen for analysis, and in fact were rather uniform as indicated by the low values of SD and coefficient of variation (Tables 1 and 2). For example, the CVs of RGB values for white flowers of upland cotton varied from 2 to 6% (Table 1). In contrast, sampling a visibly mixed colored area, such as the edge of a white flower and green foliage, gave considerably higher coefficients of variation of 30, 17, and 36% (182 ± 51, 207 ± 35, 149 ± 59, respectively; $n = 1{,}406$), as could be expected. The RGB values are important in reproducing the mean color, whereas the SD and coefficient of variation specify how uniform the original color was. However, ambient light and camera exposure can influence the RGB values as shown for the green lacewing at different light exposures (Table 2). This effect can be minimized by taking a percentage of each component relative to all three. The lacewing RGB values varied considerably due to exposure, but the trichromatic percentages of the RGB varied less, indicating that the percentages are a more consistent measure of the color. The variations in the "solid" colors of the insects (Table 2) were somewhat more than in the lacewing, with the cerambycid beetle having the largest SDs. The method applied to callow and mature adults of a bark beetle, *Ips paraconfusus* Lanier (Coleoptera: Scolytidae), clearly discriminate differences in maturation (Table 2). Two batches of yellow plastic sheets used in sticky traps were obtained in different years from the manufacturer and seemed to be slightly different shades to the eye and analysis of their images showed the RGB values were different (Table 2).

The software draws a graph under the uploaded image after an area is selected, such as an area on a "crimson-purple" adelgid gall on Engelmann spruce (Fig. 2). The graph reports the RGB values, SD, coefficient of variation, and the trichromatic component percentages. It is apparent that the colors of the flowers and leaves of different species and varieties of cotton form different groups as plotted on the color-space hexagon (Fig. 3). The plotting of the same color data in a two-dimensional (2D)-cubic representation (Fig. 4) gave somewhat different results from the hexagon method. Lines were drawn from the data points to the floor of the cube to help in perceiving the spatial patterns. The ternary plot of the data gave results (Fig. 5) that were spatially similar to the first two methods although the patterns were geometrically different.

A *t*-test was used to compare a mean within-group distance to a mean intergroup distance to test whether two groups were significantly separated in RGB true-3D color space. The colors of newly opened yel-

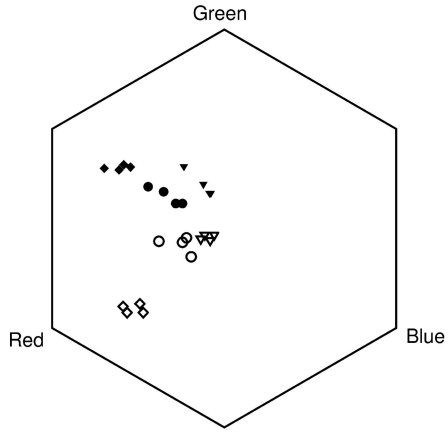

Fig. 3. Hexagon color space mapping of cotton leaves and flowers. Colors of white flowers of *G. hirsutum* are represented by filled circles, 1-d-old white flowers by open circles, yellow flowers of *G. barbadense* by filled diamonds, red flowers of *G. hirsutum* by open diamonds, green leaves of *G. hirsutum* (having white flowers) by filled triangles, and brownish red-green leaves of *G. hirsutum* (having red flowers) by open triangles (see text for details).

lowish white flowers of upland cotton formed a group with a mean within-group distance (WG) of 25.2 color-units that was similar to the same 1-d-old flowers that became pinkish overnight (WG = 30.4). These two groups had a mean between-groups distance (BG) of 60.5 that indicated they were spaced apart significantly in the color space ($t = 5.44$, df = 20, $P < 0.001$) (Table 1). The white flowers of upland cotton also were separated from the yellow flowers of Pima cotton (WG = 25.3, BG = 75.7, $t = 5.57$, df = 20, $P < 0.001$). The green leaves of upland cotton (WG = 59.5) were distinct in color from its red variety (WG = 32.3, BG = 113.9, $t = 3.69$, df = 20, $P = 0.001$) but not from the Pima cotton species (WG = 31.2, BG = 42.7, $t = 1.72$, df = 20, $P = 0.1$). In Table 2, the darker forest green of the ventral abdomens of female *L. hesperus* bugs (WG = 28.2) and the yellow-green of males (WG = 37.9) were significantly different in color (BG = 86.0, $t = 4.12$, df = 20, $P < 0.001$).

Variation in digital cameras could be a significant drawback to the analysis method. However, the variation in RGB values of purple or red paper among five digital camera models was reasonably consistent (Table 3). In addition, as mentioned, trichromatic percentages showed even less variation among the cameras. The RGB software method was compared with reflectance spectrograms from the USB2000 spectroradiometer for two batches of yellow plastic sheets used in insect-traps. The results showed different RGB values as well as distinct spectral curves (Fig. 6), indicating both methods are sensitive in detecting subtle differences in color. Reflected colors from a typical bright yellow-white flower and a green leaf of upland cotton were analyzed by the RGB method and corresponded well to spectrograms taken by the USB2000 of the same material (Fig. 7).

Some differences in the maximum number of colors that can be plotted among the three color-space models (hexagon, 2D-cube, and ternary diagrams) were discovered. I calculated that some RGB colors will plot to the same location, for example, in the ternary diagram RGB values of 20, 60, and 30 are redundant with 40, 120, and 60. Because the three dimensional values are compressed onto a 2D surface in all three diagrams, many values are hidden behind others. In a simple color system with only four intensity shades of each component of RGB (e.g., R is an integer from 0 to 3), there are $4^3 = 64$ colors. Plotting these in the hexagon, 2D-cube, or ternary diagrams would not give 64 positions but somewhat less, in fact, 37, 46, and 49 positions, respectively. Generating all possible combinations of RGB values is done with three nested loops in BASIC (FOR R = 0–255 : FOR G = 0–255 : FOR B = 0–255 : NEXT : NEXT : NEXT) with the resulting values converted to x, y coordinates (as de-

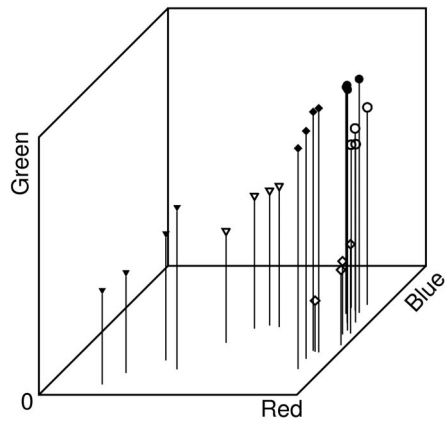

Fig. 4. 2D-cube color space mapping of cotton leaves and flowers. Point representations as described in Fig. 3.

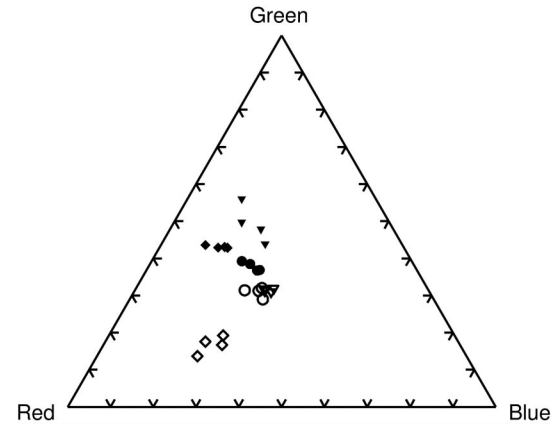

Fig. 5. Ternary color space mapping of cotton leaves and flowers. Point representations as described in Fig. 3.

Table 3. Mean RGB values and trichromatic percentages from areas of digital photos of purple and red construction paper taken with five digital camera models

Digital camera	Pixels[a]	R ± SD (CV) R %[b]	G ± SD (CV) G %	B ± SD (CV) B %
Purple construction paper in sunlight				
Nikon Coolpix 2100	2,160	182 ± 2 (1) 33.1	139 ± 2 (1) 25.3	229 ± 2 (1) 41.6
Canon Power-Shot G3	2,160	158 ± 3 (2) 31.2	123 ± 3 (2) 24.3	225 ± 3 (1) 44.5
Nikon Coolpix 990	2,160	174 ± 3 (2) 32.2	150 ± 3 (2) 27.8	216 ± 3 (1) 40.0
Olympus D-340R	2,160	176 ± 3 (2) 32.9	142 ± 3 (2) 26.5	217 ± 3 (1) 40.6
Nikon D70 SLR	2,160	154 ± 2 (2) 31.7	132 ± 3 (2) 27.2	200 ± 2 (1) 41.2
Red construction paper in sunlight				
Nikon Coolpix 2100	2,160	238 ± 2 (1) 61.2	62 ± 2 (3) 15.9	89 ± 3 (3) 22.9
Canon Power-Shot G3	2,160	239 ± 2 (1) 60.8	69 ± 2 (3) 17.6	85 ± 2 (3) 21.6
Nikon Coolpix 990	2,160	235 ± 2 (1) 57.0	80 ± 2 (2) 19.4	97 ± 2 (3) 23.5
Olympus D-340R	2,160	235 ± 2 (1) 57.9	76 ± 2 (2) 18.8	95 ± 2 (3) 23.4
Nikon D70 SLR	2,160	225 ± 1 (1) 62.2	62 ± 2 (3) 17.1	75 ± 2 (2) 20.7

[a] Area analyzed in pixels (n of sample).
[b] Represents the R (red intensity) ± SD (standard deviation) [CV, coefficient of variation defined as SD/R × 100) and percent red (R/(R + G + B) × 100]. G and B defined similarly.

scribed above). If the x, y coordinates are unique they are stored at the end of a growing array list. When all combinations are tested, the length of the array then describes the number of values that can be uniquely plotted. Table 4 shows the number of color combinations (n) for various numbers of intensities of RGB components (from 2 to 12) for the three methods. The hexagon and 2D-cube plots show up as a geometric series and are solved for the hexagon as follows:

$$n = 1 + \sum_{j=1}^{255} 6j \qquad [3]$$

and for the 2D-cube as

$$n = 1 + \sum_{j=1}^{255} 8j - 1 \qquad [4]$$

where j varies up to the number of intensities of interest minus 1. Thus, at the usual RGB values of 256 component intensities there are 195,841 unique plots for the hexagon (equation 3) and 260,866 nonredundant positions for the 2D-cube (equation 4). The ternary diagram is clearly superior to these methods, because many more positions seem available. The sequence was computed up to 32 intensities (27,133 unique positions) and seemed erratic (Table 4). The percentage of unique values at all intensity steps was ≈80% of the cubed value at all steps in the sequence, which predicts a value of ≈13.4 million positions in the ternary diagram at 256 shades of RGB components.

Discussion

The description of color in entomological research pertains to objects that reflect colors detected by visual systems of humans, insects, and digital cameras. The RGB analysis software provides a simple, inexpensive, and objective method to portray and analyze colors in images captured by commonly available digital cameras. The method is useful because descriptions of colors are subjective and vary due to cultural and language influences (Zollinger 1988, Saunders and van Brakel 1989, Mausfeld 2003). In addition, researchers commonly differ in color reception of their

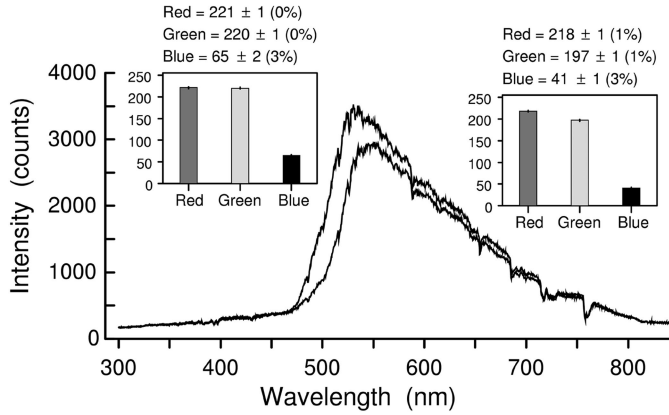

Fig. 6. Overlaid spectrograms (USB2000 spectroradiometer) of sunlight reflected from each of two yellow plastic sheets used in insect traps. The left inset of RGB values corresponds to the first sheet A with its spectrum shown offset to the left and higher, whereas the second sheet B corresponds to the inset on the right with a spectrum shifted to the right and slightly lower (RGB analysis of images taken by Nikon 2100, 18 February 2005 at 1130 hours, yellow sheets as in Table 2).

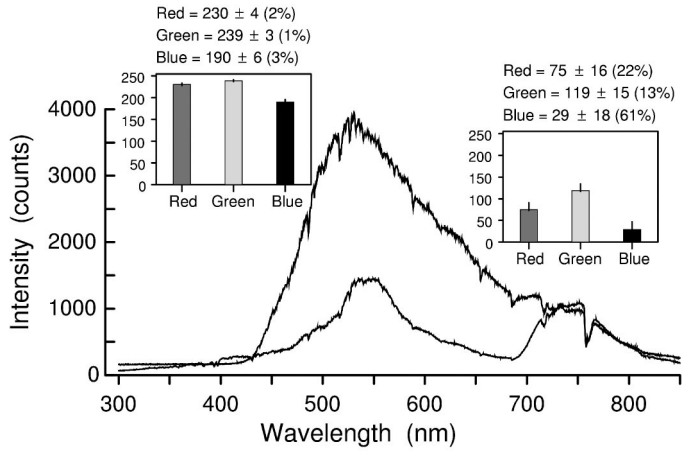

Fig. 7. Overlaid spectrograms (USB2000 spectroradiometer) of sunlight reflected off a white-yellow flower (top spectrum) and a green leaf (bottom spectrum) of upland cotton. The left inset of RGB values corresponds to the cotton flower, whereas the right inset corresponds to the green leaf (RGB analysis of images taken by Nikon 2100, 5 June 2005 at 1100 hours).

cone pigment opsins. Approximately 6–8% of men are red-green color deficient because they have only a green or a red opsin gene, whereas ≈0.1% of both sexes have no blue opsin (λ_{max} 426 nm; Went and Pronk 1985, Merbs and Nathans 1992). Both the gene that codes for green opsin (maximum absorbance, λ_{max}, at 530 nm) and the polymorphic gene for red opsin (λ_{max} of either 552 or 557 nm) are on the X-chromosome (Onishi et al. 2002, Deeb et al. 2003). In a group of 50 normal Caucasian males, 62% had serine at amino acid position 180 in their red opsin (λ_{max} 557 nm), whereas 38% had alanine instead, causing absorption to shift to 552 nm (Merbs and Nathans 1992, Winderickx et al. 1992). The group with red opsin of 552 nm was less sensitive to differences in yellow-orange hues in a Rayleigh color-matching test. Females have two X-chromosomes and thus are either homozygous 552 nm (15%) or 557 nm (38%), or heterozygous (47%), as confirmed on color matching tests.

Another reason to use the RGB method to describe colors accurately is that insects perceive colors as well, although with a different set of color receptors than humans. All insect orders seem to have UV receptors (345–360 nm), whereas probably all holometabolous insects have at least trichromatic vision with an additional blue receptor (400–450) and a green (515–540) or red (575) receptor (Stark and Wasserman 1972, Laughlin 1976, Menzel and Blakers 1976, Smola and Meffert 1979, Ichikawa and Tateda 1982, Chittka 1997, Kevan et al. 2001, Briscoe et al. 2003). Some species in Lepidoptera, Odonata, and Hymenoptera seem to have tetrachromatic vision, or even five or more color receptors (Kretz 1979, Kelber et al. 2001, Briscoe et al. 2003). The number of major colors in humans and insects with trichromatic vision is $2^3 = 8$, whereas in tetrachromats it is $2^4 = 16$, the perceptions of the latter type being difficult to comprehend. The insect UV receptor probably evolved in their ancestors >570 million years ago under different atmospheric conditions with more UV and blue light than today (Chittka 1996, 1997; Kevan et al. 2001). Flowers of angiosperm plants occurred some 300 million years after insects became dominant on earth and as such have evolved flower colors that contrast with green leaves (Table 1;

Table 4. Number of unique x, y positions for various numbers of integer RGB component intensities plotted in various color space methods

Component intensities[a]	3D color combinations[b]	Hexagon color space[c]	2D-cube color space[c]	Ternary color space
2	8	7	8	7
3	27	19	23	19
4	64	37	46	49
5	125	61	77	91
6	216	91	116	175
7	343	127	163	253
8	512	169	218	415
9	729	217	281	571
10	1,000	271	352	805
11	1,331	331	431	1,033
12	1,728	397	518	1,423
256	16,777,216	195,841	260,866	$\approx 13.4 \times 10^6$

[a] Intensity values of RGB for each component from 0 to 1 less than value shown.
[b] Color combinations of the respective intensity values are equal to the cube of the number of component intensity values.
[c] Sequences were found empirically and could be calculated from summation equations 3 and 4 in text.

Fig. 7) and coincide with the insect vision system, especially among bees (Chittka 1996, 1997). Insects may have evolved their bright colors (e.g., Table 3) not only for aposematic warnings primarily against vertebrates (Boeve and Pasteels 1985, Malcolm 1989, Aliabadi et al. 2002) but also for recognition of competitors (territoriality) and mates (Bernard and Remington 1991, Silberglied 1989, Jiggins et al. 2001). Insects also respond to color in the visible and UV wavelengths reflected from their host plants (Harris et al. 1993, Picaud et al. 2002, Hirota and Kato 2004). Thus, humans may be unaware of many critical aspects of natural coloration and perception by insects (and vice versa) because of different sets of color receptors.

Besides insect and vertebrate visual systems, a third system that is important in color description is that of the digital camera. Images taken with different cameras vary somewhat in RGB component values, although percentages of each component vary less (Table 3). Future technological advances are expected to minimize such color differences between cameras. The digital camera has a charge-coupled device (CCD) that is an array of capacitors (corresponding to pixels) that respond to light from 300 to 1000 nm, but blue, red, and two green filters for each pixel reduces this range to approximately the human range of 400–700 nm (Wetzel and Des Jardin 1999, Des Jardin 2002). However, the digital camera wavelength sensitivity can include the insect UV-sensitive range, at least in part, and all of the far-red vision range of humans and insects. Spectroradiometers (e.g., Ocean Optics) use a CCD and a diffraction grating to measure intensities of narrow bands of wavelengths over the whole range, whereas the camera CCD arrays average, broaden, and partition the wavelengths into the three color values as do the insect and human opsin receptors that usually have SDs of 40–60 nm (Menzel and Blakers 1976, Langer et al. 1979, Schlecht 1979, Ichikawa and Tateda 1982, Merbs and Nathans 1992, Kelber et al. 2001, Kevan et al. 2001).

Spectroradiometers provide a graphical analysis of reflected light from colored objects that are usually larger than insects (Figs. 6 and 7). In contrast, RGB values or their trichromatic percentages obtained by digital cameras can be used to describe as well as reproduce colors by computer monitor or printer. If desired, the RGB values can be converted to other color systems such as HSB (hue, saturation, and brightness) with the Internet software (Utility in Fig. 1; Baxes 1994). One major disadvantage of spectroradiometers similar to that used here is that they average reflected light from an ill-defined area, comprised of a mixture of angles from many variously colored areas of the insect. In contrast, the digital camera can discriminate small colored areas of just a few pixels, especially if viewed through a macro lens. The software also allows measurement of the variation in the pixel sources of light that a spectroradiometer only averages. Another problem with spectroradiometers is that their wavelength spectrum of intensities (Figs. 6 and 7) is not intuitively understood as a color (although in principle algorithms could convert the spectrum to a color), whereas RGB values are easy to convert to colors with any paint program.

Digital cameras today have adequate resolution for color image analysis. For example, inexpensive 2-megapixel cameras can take photos of 1,600 by 1,200 pixels, which is comparable to a resolution of 1-mm per pixel over a 1.6- by 1.2-m area. Over an area of 16 by 12 cm that is reasonable for flower or leaf photos, the resolution compares to 0.1 mm per pixel (100 pixels per mm^2). At a macro level of 1.6 by 1.2 cm for insect photography, the resolution is 0.01 mm (10 μm). Still higher resolution is possible through a compound microscope. The accurate description of color changes in an object over time during growth and development is optimized by using the same camera under constant light conditions. The software for analysis of color pixel areas in digital images should prove useful as an objective, quantitative, statistical, and standardized method to describe colors of insects, plants, and other research objects such as insect monitoring traps.

Acknowledgments

I thank L. Elhoff, L. Jech, D. Langhorst, P. Alexander, and B. Hefner for technical assistance in maintaining colonies of cotton insects and plants. J. Blackmer and L. Lee provided the plastic sheeting. I also thank J. Blackmer, H. Flint, and several anonymous reviewers of the manuscript.

References Cited

Aliabadi, A., J.A.A. Renwick, and D. W. Whitman. 2002. Sequestration of glucosinolates by harlequin bug *Murgantia histrionica.* J. Chem. Ecol. 28: 1749–1762.

Appleby, J. H., and P. F. Credland. 2001. Bionomics and polymorphism in *Callosobruchus subinnotatus* (Coleoptera: Bruchidae). Bull. Entomol. Res. 91: 235–244.

Baxes, G. A. 1994. Digital image processing. Wiley, Inc., New York.

Bernard, G. D., and C. L. Remington. 1991. Color vision in *Lycaena* butterflies: spectral tuning of receptor arrays in relation to behavioral ecology. Proc. Natl. Acad. Sci. U.S.A. 88: 2783–2787.

Blackmer, J. L., C. Rodriguez-Saona, J. A. Byers, K. L. Shope, and J. P. Smith. 2004. Behavioral response of *Lygus hesperus* to conspecifics and headspace volatiles of alfalfa in a Y-tube olfactometer. J. Chem. Ecol. 30: 1547–1564.

Boeve, J. L., and J. M. Pasteels. 1985. Modes of defense in nematine sawfly larvae: efficiency against ants and birds. J. Chem. Ecol. 11: 1019–1036.

Bohac, J. R., D. M. Jackson, J. D. Mueller, and P. D. Dukes, Sr. 2002. 'Ruddy': a multiple-pest-resistant sweetpotato. Hortscience 37: 993–994.

Braendle, C., and W. W. Weisser. 2001. Variation in escape behavior of red and green clones of the pea aphid. J. Insect Behav. 14: 497–509.

Briscoe, A. D., G. D. Bernard, A. S. Szeto, L. M. Nagy, and R. H. White. 2003. Not all butterfly eyes are created equal: rhodopsin absorption spectra, molecular identification, and localization of ultraviolet-, blue-, and green-sensitive rhodopsin-encoding mRNSs in the retina of *Vanessa cardui.* J. Comp. Neurol. 458: 334–349.

Byers, J. A. 1992. Dirichlet tessellation of bark beetle spatial attack points. J. Anim. Ecol. 61: 759–768.

Byers, J. A. 1996. Taxokey: a universal taxonomic key program using DOS text files and graphics. Comp. Appl. Biosci. 12: 185–189.

Byers, J. A. 2002. Internet programs for drawing moth pheromone analogs and searching literature database. J. Chem. Ecol. 28: 807–817.

Chittka, L. 1996. Optimal sets of color receptors and color opponent systems for coding of natural objects in insect vision. J. Theor. Biol. 181: 179–196.

Chittka, L. 1997. Bee color vision is optimal for coding flower color, but flower colors are not optimal for being coded – why? Israel J. Plant Sci. 45: 115–127.

Deeb, S. S., M. J. Wakefield, T. Takashi, L. Marotte, S. Yokoyama, and J. A. Marshall Graves. 2003. The cone visual pigments of an Australian marsupial, the tammar wallaby (*Macropus eugenii*): sequence, spectral tuning, and evolution. Mol. Biol. Evol. 20: 1642–1649.

Des Jardin, W. 2002. CCDs make the most of every photon. Photonics Spectra (August), Laurin Publishing Co. Inc., Pittsfield, MA.

Goodman, D. 1996. Danny Goodman's JavaScript handbook. IDG Books Worldwide, Inc., Foster City, CA.

Harris, M. O., S. Rose, and P. Malsch. 1993. The role of vision in the host plant-finding behaviour of the Hessian fly. Physiol. Entomol. 18: 31–42.

Hirota, T., and Y. Kato. 2004. Color discrimination on orientation of female *Eurema hecabe* (Lepidoptera: Pieridae). Appl. Entomol. Zool. 39: 229–233.

Hoback, W. W., T. M. Svatos, S. M. Spomer, and L. G. Higley. 1999. Trap color and placement affects estimates of insect family-level abundance and diversity in a Nebraska salt marsh. Entomol. Exp. Appl. 91: 393–402.

Howarth, V.M.C., and F. G. Howarth. 2000. Attractiveness of methyl eugenol-baited traps to oriental fruit fly (Diptera: Tephritidae): effects of dosage, placement, and color. Proc. Hawaiian Entomol. Soc. 34: 187–198.

Ichikawa, T., H. Tateda. 1982. Distribution of color receptors in the larval eyes of four species of Lepidoptera. J. Comp. Physiol. 149: 317–324.

Jiggins, C. D., R. E. Nalsbit, R. L. Coe, and J. Mallet. 2001. Reproductive isolation caused colour pattern mimicry. Nature (Lond.) 411: 302–305.

Kelber, A., C. Thunell, and K. Arikawa. 2001. Polarisation-dependent colour vision in *Papilio* butterflies. J. Exp. Biol. 204: 2469–2480.

Kelley, K. M., B. K. Behe, J. A. Biernbaum, and K. L. Poff. 2002. Combinations of colors and species of containerized edible flowers: effect on consumer preferences. HortScience 37: 218–221.

Kevan, P. G., L. Chittka, and A. G. Dyer. 2001. Limits to the salience of ultraviolet: lessons from colour vision in bees and birds. J. Exp. Biol. 204: 2571–2580.

Kretz, R. 1979. A behavioural analysis of colour vision in the ant *Cataglyphis bicolor* (Formicidae, Hymenoptera). J. Comp. Physiol. 131: 217–233.

Langer, H., B. Hamann, and C. C. Meinecke. 1979. Tetrachromatic visual system in the moth *Spodoptera exempta* (Insecta: Noctuidae). J. Comp. Physiol. 129: 235–239.

Laughlin, S. B. 1976. The sensitivities of dragonfly photoreceptors and the voltage gain of transduction. J. Comp. Physiol. 111: 221–247.

Malcolm, S. B. 1989. Disruption of web structure and predatory behavior of a spider by plant-derived chemical defenses of an aposematic aphid. J. Chem. Ecol. 15: 1699–1716.

Marchand, D., and J. N. McNeil. 2004. Avoidance of intraspecific competition via host modification in a grazing, fruit-eating insect. Anim. Behav. 67: 397–402.

Mausfeld, R. 2003. Colour perception. Oxford University Press, Oxford, United Kingdom.

Menzel, R., and M. Blakers. 1976. Colour receptors in the bee eye – morphology and spectral sensitivity. J. Comp. Physiol. 108: 11–33.

Merbs, S. L., and J. Nathans. 1992. Absorption spectra of human cone pigments. Nature (Lond.) 356: 433–435.

Onishi, A., S. Koike, M. Ida-Hosonuma, H. Imai, Y. Shichida, O. Takenaka, A. Hanazawa, H. Komatsu, A. Mikami, S. Goto, et al. 2002. Variations in long- and middle-wavelength-sensitive opsin gene loci in crab-eating monkeys. Vis. Res. 42: 281–292.

Picaud, F., V. Gloaguen, D. Petit. 2002. Mechanistic aspects to feeding preferences in *Chorthippus binotatus* (Acrididae, Gomphocerinae). J. Insect Behav. 15: 513–526.

Saunders, B.A.C., and J. van Brakel. 1989. On cross-cultural colour semantics. Int. J. Moral Soc. Stud. 4: 173–180.

Schlecht, P. 1979. Colour discrimination in dim light: an analysis of the photoreceptor arrangement in the moth *Deilephila.* J. Comp. Physiol. 129: 257–267.

Silberglied, R. E. 1989. Visual communication and sexual selection among butterflies, pp. 207–221. *In* R. I. Vane-Wright and P. R. Ackery [eds.], The biology of butterflies. Princeton University Press, Princeton, NJ.

Smola, U., and P. Meffert. 1979. The spectral sensitivity of the visual cells R7 and R8 in the eye of the blowfly *Calliphora erythrocephala.* J. Comp. Physiol. 133: 41–52.

Sokal, R. R., and F. J. Rohlf. 1995. Biometry, 3rd ed. W.H. Freeman and Company, New York.

Stanek, W. R. 1996. HTML, CGI, SGML, VRML, JAVA Web publishing unleashed. Sams.net Publishing, Indianapolis, IN.

Stark, W. S., and G. S. Wasserman. 1972. Transient and receptor potentials in the electroretinogram of *Drosophila.* Vis. Res 12: 1771–1775.

Tanaka, S. 2000. The role of [His^7]-corazonin in the control of body-color polymorphism in the migratory locust, *Locusta migratoria* (Orthoptera: Acrididae). J. Insect Physiol. 46: 1169–1176.

Trzoniec, S. 2005. How to choose your new camera. PC How-To Guide, Digital Photography. Harris Publ., Inc. 3: 12–15.

Wang, Q. 2002. Sexual selection of *Zorion guttigerum* Westwood (Coleoptera: Cerambycidae: Cerambycinae) in relation to body size and color. J. Insect Behav. 15: 675–687.

Went, L. N., and N. Pronk. 1985. The genetics of tritan disturbances. Hum. Genet. 69: 255–262.

Wetzel, K., and B. Des Jardin. 1999. Image sensors: more sensitivity increases options. Photonics Spectra (February), Laurin Publishing Co. Inc.. Pittsfield, MA.

Whitney, K. D., and M. L. Stanton. 2004. Insect seed predators as novel agents of selection on fruit color. Ecology 85: 2153–2160.

Winderickx, J., D. T. Lindsey, E. Sanocki, D. Y. Teller, A. G. Motulsky, and S. S. Deeb. 1992. Polymorphism in red photopigment underlies variation in colour matching. Nature (Lond.) 356: 431–433.

Zhao, J. T., C. L. Bennett, G. J. Stewart, M. Frommer, and K. A. Raphael. 2003. The scarlet eye colour gene of the tephritid fruit fly: *Bactrocera tryoni* and the nature of two eye colour mutations. Insect Mol. Biol. 12: 263–269.

Zollinger, H. 1988. Categorical color perception: influence of cultural factors on the differentiation of primary and derived basic color terms in color naming by Japanese children. Vis. Res. 28: 1379–1382.

Received 8 June 2005; accepted 29 April 2006.